AGU PUBLICATIONS

JGR

Journal of Geophysical Research: Space Physics

RESEARCH ARTICLE
10.1002/2015JA022166

Key Points:
- The ionosphere behaves incompressibly, moving upward when the magnetosphere is compressed.
- Eveningtime SC electric fields are anomalously enhanced in the same direction as in the daytime
- SC electric fields are potential fields transmitted with the ionospheric currents.

Correspondence to:
T. Kikuchi,
kikuchi@stelab.nagoya-u.ac.jp

Citation:
Kikuchi, T., K. K. Hashimoto, I. Tomizawa, Y. Ebihara, Y. Nishimura, T. Araki, A. Shinbori, B. Veenadhari, T. Tanaka, and T. Nagatsuma (2016), Response of the incompressible ionosphere to the compression of the magnetosphere during the geomagnetic sudden commencements, *J. Geophys. Res. Space Physics*, *121*, doi:10.1002/2015JA022166.

Received 13 NOV 2015
Accepted 30 DEC 2015
Accepted article online 11 JAN 2016
Corrected 20 FEB 2016

This article was corrected on 20 FEB 2016. See the end of the full text for details.

Response of the incompressible ionosphere to the compression of the magnetosphere during the geomagnetic sudden commencements

T. Kikuchi[1,2], K. K. Hashimoto[3], I. Tomizawa[4], Y. Ebihara[2], Y. Nishimura[5], T. Araki[6], A. Shinbori[2], B. Veenadhari[7], T. Tanaka[8], and T. Nagatsuma[9]

[1]Institute for Space-Earth Environmental Research, Nagoya University, Nagoya, Japan, [2]Research Institute for Sustainable Humanosphere, Kyoto University, Kyoto, Japan, [3]School of Agriculture, Kibi International University, Minamiawaji, Japan, [4]Center for Space Science and Radio Engineering, University of Electro-Communications, Chofu, Japan, [5]Department of Atmospheric and Oceanic Sciences, University of California, Los Angeles, California, USA, [6]Geophysical Institute, Kyoto University, Kyoto, Japan, [7]Indian Institute of Geomagnetism, New Mumbai, India, [8]International Center for Space Weather Science and Education, Kyushu University, Fukuoka, Japan, [9]National Institute of Information and Communications Technology, Koganei, Japan

Abstract The ionospheric plasma in midlatitude moves upward/downward during the geomagnetic sudden commencement causing the HF Doppler frequency changes; SCF (+ −) and (− +) on the dayside and nightside, respectively, except for the SCF (+ −) in the evening as found by Kikuchi et al. (1985). Although the preliminary and main frequency deviations (PFD, MFD) of the SCF have been attributed to the dusk-to-dawn and dawn-to-dusk potential electric fields, there still remain questions if the positive PFD can be caused by the compressional magnetohydrodynamic (MHD) wave and what causes the evening anomaly of the SCF. With the HF Doppler sounder, we show that the dayside ionosphere moves upward toward the Sun during the main impulse (MI) of the SC, when the compressional wave is supposed to push the ionosphere downward. The motion of the ionosphere is shown to be correlated with the equatorial electrojet, matching the potential electric field transmitted with the ionospheric currents from the polar ionosphere. We confirmed that the electric field of the compressional wave is severely suppressed by the conducting ionosphere and reproduced the SC electric fields using the global MHD simulation in which the potential solver is employed. The model calculations well reproduced the preliminary impulse and MI electric fields and their evening anomaly. It is suggested that the electric potential is transmitted from the polar ionosphere to the equator by the zeroth-order transverse magnetic (TM0) mode waves in the Earth-ionosphere waveguide. The near-instantaneous transmission of the electric potential leads to instantaneous global response of the incompressible ionosphere.

1. Introduction

When the solar wind shock hits the magnetosphere, the magnetopause currents are intensified transiently around the subsolar point. The intensified magnetopause currents launch stepwise/impulsive magnetic perturbations which propagate toward the Earth with the compressional magnetohydrodynamic (MHD) waves and appear as the geomagnetic sudden commencement (SC) on the ground [*Tamao*, 1964; *Wilken et al*., 1982]. The stepwise increase in the H component magnetic field at low latitudes is referred to as DL (disturbances at low latitude) [*Araki*, 1977]. The compressional MHD waves carry the westward electric field at all local times in the magnetosphere causing the earthward motion of the magnetospheric plasma [*Shinbori et al*., 2004].

The localized intensification of the magnetopause currents generates electric potentials which are transmitted with the field-aligned currents (FACs) by the transverse (Alfven) waves down the magnetic field lines to the polar ionosphere [*Tamao*, 1964]. After arriving at the polar ionosphere, the electric potentials excite the zeroth-order TM (TEM:transverse electromagnetic) mode wave in the Earth-ionosphere waveguide, which propagates to the low-latitude ionosphere at the speed of light [*Kikuchi et al*., 1978; *Kikuchi and Araki*, 1979b]. The electric potential is positive in the afternoon and negative in the morning. The dusk-to-dawn electric field drives two-cell Hall current vortices in high-middle latitudes and causes the preliminary impulse (PI) with the timescale of 1 min with negative polarity (PRI: preliminary reverse impulse) in the afternoon and positive polarity (PPI: preliminary positive impulse) in the morning [*Nagata and Abe*, 1955]. The two-cell current pattern of the PI is similar to those of

the quasiperiodic DP2 currents driven by fluctuations of the southward interplanetary magnetic field [*Nishida et al*., 1966; *Nishida*, 1968]. The electric field drives the Pedersen currents flowing into the equatorial ionosphere where the currents (EEJ) are intensified by the Cowling effect [*Hirono*, 1952; *Baker and Martyn*, 1953]. As a result, the PRI appears on the dayside and PPI on the nightside at the equator [*Araki et al*., 1985]. In the context of current circuit, the EEJ is connected with the FACs by the Pedersen currents in midlatitudes. As a result, the PRI/PPI appears at high latitude and equator simultaneously within the temporal resolution of observation, say, 10 s [*Araki*, 1977; *Kikuchi*, 1986].

One minute later, the directions of the electric field and currents are reversed during the main impulse (MI) of the SC, leading to that the SC appears as SC (− +) and (+ −) at high latitudes in the afternoon and morning, respectively. The MI currents are intensified at the dayside equator in the same way as the PI, resulting in the equatorial enhancement of the SC. The electric potentials and field-aligned currents for the PI and MI have been reproduced by the global MHD simulations [*Slinker et al*., 1999; *Fujita et al*., 2003a, 2003b; *Tanaka*, 2007]. The dynamo for the PI currents is located close to the magnetopause [*Fujita et al*., 2003a], while the MI currents are generated first by the compressional waves and then by the dynamo similar to that of the Region 1 field-aligned currents [*Fujita et al*., 2003b].

The magnetic perturbations due to the ionospheric currents, DP (PI) and DP (MI), are superimposed on the DL. Thus, the ground magnetic perturbations become somewhat complicated but are well understood as a superposition of the DL, DP(PI), DP(MI) [*Araki*, 1994], and Biot-Savart effects of the FACs [*Kikuchi and Araki*, 1985; *Kikuchi et al*., 2001; *Araki et al*., 2006; *Shinbori et al*., 2009]. The amplitude of PI decreases as the DL becomes dominant in middle-low latitudes, while the DL is superimposed on by the PI and MI with substantial amplitude at the dayside equator and small PPI and negative MI at the nightside equator.

The electric fields of the SC have been observed with the HF Doppler sounders in midlatitudes [*Davies et al*., 1962; *Kanellakos and Villard*, 1962; *Chan et al*., 1962; *Huang et al*., 1973, 1976; *Kikuchi et al*., 1985; *Kikuchi*, 1986]. The SC-associated HF Doppler frequency deviations (SCF) are mostly in a bipolar structure, SCF (+ −) and SCF (− +), although single impulses, SCF (+) and SCF (−) are also observed [*Huang et al*., 1973]. The positive preliminary frequency deviation (PFD) of SCF (+ −) was explained in terms of the inductive electric field inversely proportional to the rise time of the SC, which had been carried by the compressional MHD wave [*Huang et al*., 1976]. Later, *Kikuchi et al*. [1985] found that SCF (+ −) appears in the daytime and evening and SCF (− +) in the nighttime and suggested that the PFD and MFD (main frequency deviation) are caused by the dusk-to-dawn and dawn-to-dusk electric fields associated with the ionospheric currents of the PI and MI, respectively, except for the evening SCF (+ −). Furthermore, *Kikuchi* [1986], using the high time resolution HF Doppler and magnetometer data, found that the negative PFD in the nighttime occurred simultaneously (within 10 s) with the PI at high latitude. The simultaneous onset of the PFD and high latitude PI is direct evidence for the near-instantaneous transmission of the PI electric field from the polar ionosphere to the nightside low latitude similar to the dayside PRI [*Araki*, 1977]. The electric fields being in reversed direction on the dayside and nightside are consistent with the potential field like the DP2 carried by the field-aligned currents to the polar ionosphere. Based on the model calculations of the global distribution of the electric potential with an input of field-aligned currents in the polar ionosphere, *Tsunomura* [1999] pointed out that the evening anomaly of the SC electric fields could be derived from the asymmetric distribution of the electric potential due to the Hall effects and day-night inhomogeneity of the ionospheric conductivity.

The local time distribution of the electric field with the anomalous appearance of the SCF (+ −) in the evening and the instantaneous transmission of the PI electric field to low latitude have been confirmed with the electric field measurements on board the low-Earth orbiting satellite, ROCSAT-1 [*Takahashi et al*., 2015]. All the observations and model calculations seem to be in favor of the electric field transmission from the polar ionosphere. However, the electric field of the compressional MHD wave remains a possible driver of the ionospheric motion on the dayside. Actually, the positive PFD has been explained in terms of the wave electric field not only back several decades [*Huang et al*., 1976] but also fairly recently [*Pilipenko et al*., 2010]. Besides, compressive property of the ionosphere has been invoked to explain the equatorial enhancement of the SC [*Jacobs and Watanabe*, 1963] and the motion of the ionosphere during ULF pulsations [*Poole et al*., 1988; *Sutcliffe and Poole*, 1990].

In the present paper, we clarify that the SC electric fields detected with the HF Doppler sounders are not wave fields but potential fields transmitted from the polar ionosphere with the ionospheric currents and confirm

Table 1. List of the Western Pacific, Brazilian, and African Magnetometer Stations and HF Doppler Sounders in Japan

	GLAT	GLON	MLAT	MLON	LT = UT+	DIST	EL ANGLE
	(deg)	(deg)	(deg)	(deg)	(h)	(km)	(deg)
			MAG Station				
KAK, Kakioka, Japan	36.23	140.18	27.19	208.78	+9		
KNY, Kanoya, Japan	31.42	130.88	21.72	200.79	+9		
OKI, Okinawa, Japan	26.78	128.25	16.95	198.69	+9		
YAP, Yap, Micronesia	9.49	138.17	0.51	209.45	+9		
SLZ, Sao Luiz, Brazil	−2.60	−44.20	5.94	28.56	−3		
SMA, Santa Maria, Brazil	−29.72	−53.72	−20.35	17.49	−4		
AAE, Addis Ababa	9.04	38.77	5.35	112.53	+3		
TAM, Tamanrasset	22.79	5.53	24.30	82.32	+1		
			HFD Station				
CHF, Chofu, Japan (TX)	35.65	139.55	26.57	208.28			
ORI, Oarai, Japan (RX)	36.33	140.59	27.33	209.14		120	78.2
SGD, Sugadaira, Japan (RX)	36.52	138.32	27.33	207.07		146	75.7

that the evening anomaly is an aspect of the global distribution of the electric potentials. Addressing these issues addresses another question whether the ionosphere is compressible or incompressible. In the following sections, we examine the motion of the dayside ionosphere during the MI when the compressional waves are expected to make significant effects on the ionosphere. We analyze three SC events with small or no PFD to focus on the motion of the ionosphere during the compression of the magnetosphere and one SC event with an appreciable positive PFD which appears as if it were caused by the compression of the ionosphere. As will be shown below, the dayside ionosphere never moves toward the Earth but instead moves toward the Sun during the compression of the magnetosphere, showing that the ionosphere is incompressible. To have an idea about the electric field driving the motion of the incompressible ionosphere, we examine correlations between the motion of the ionosphere and equatorial electrojets (EEJ) that represent the global ionospheric currents originating in the polar ionosphere. Furthermore, we show the evening enhancement of the PI and MI electric fields with other three SC events and suggest that the incompressible ionosphere is moved by the potential electric fields transmitted with the ionospheric currents. Applying the simplified one-dimensional propagation model [*Kikuchi and Araki*, 1979a], we confirm that the electric field of the compressional wave is severely suppressed by the conducting ionosphere. Moreover, using the global MHD simulations of *Tanaka* [1995, 2007], we reproduce a sequence of the PI and MI electric fields to confirm the potential electric fields being responsible for the ionospheric motion and evening anomaly of the electric field. Lastly, we discuss the transmission mechanism of the electric potentials to the low-latitude ionosphere by employing the magnetosphere-ionosphere-ground transmission line model [*Kikuchi*, 2014], which includes the field-aligned currents connected with the Earth-ionosphere waveguide. The instantaneous transmission of the potential fields leads to the simultaneous response of the global ionosphere, which secures the incompressibility of the ionosphere.

2. Observations

2.1. HF Doppler Sounders and Magnetometers

The HF Doppler sounders are used to observe the vertical motion of the ionosphere, which is composed of the transmitter at Chofu, Tokyo (CHF) and receivers at Oarai, Ibaraki (ORI) and Sugadaira, Nagano (SGD), Japan (geographic and magnetic coordinates are listed in Table 1). The HF Doppler frequency changes (hereafter denoted as HFD) are caused by changes in the phase path from the transmitter to the receiver via the reflection point in the *F* region ionosphere. The phase path changes due to changes in the reflection height and/or the refractive index below the reflection height. The HFD is proportional to the frequency of the radio wave when it is caused by the changes in the reflection height, while inversely proportional when the HFD is caused by changes in the refractive index below the reflection height [*Davies et al*., 1962]. Quite a few papers have shown that the HFD is proportional to the radio frequency for the SC events [*Davies et al*., 1962; *Huang et al*., 1973; *Kikuchi et al*., 1985; *Kikuchi*, 1986], geomagnetic pulsations [*Chan et al*., 1962], and substorms [*Tsutsui et al*., 1988].

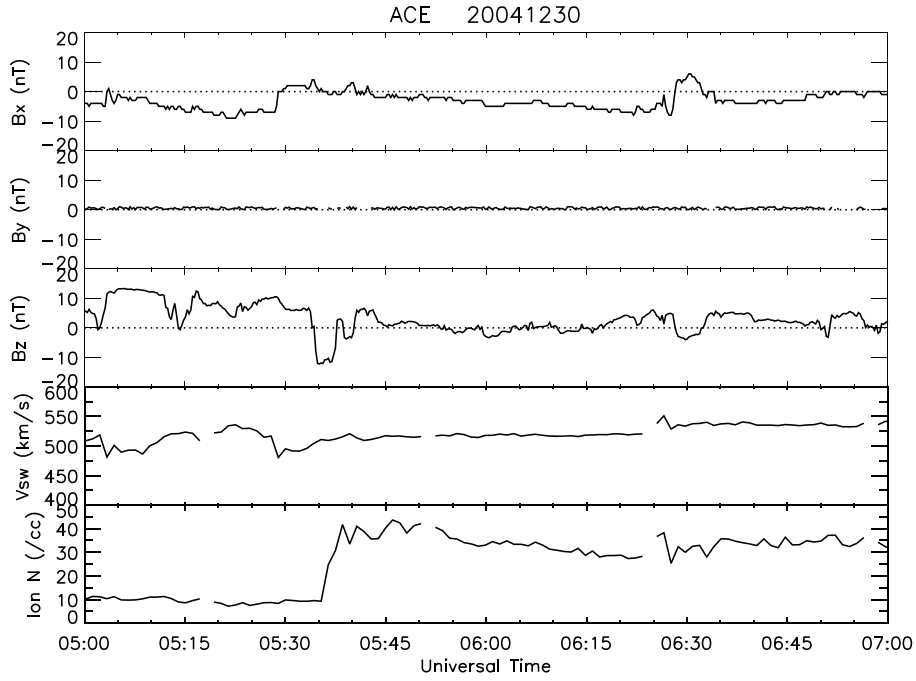

Figure 1. From the top to the bottom are plotted the interplanetary magnetic field, B_x, B_y and B_z and the solar wind velocity (V_{sw}) and density (Ion *N*) detected by ACE at L1 point for the SC event 1 on 30 December 2004. The SC was caused by the increase in *N* at 0535 UT.

Assuming that the radio wave is reflected at the height (*h*) of 300 km in the *F* region and that the *F* region plasma moves perpendicular to the electric field, ***E***, and the ambient geomagnetic field, ***B*** at the velocity, $V = E \times B/B^2$, we derive the vertical velocity, V_{vert}, and electric field, *E*, from the Doppler frequency, Δf as shown below.

$$V_{vert} = -\frac{c}{2f\sin\theta}\Delta f \tag{1}$$

$$E = -\frac{cB}{2f\cos I\sin\theta}\Delta f \tag{2}$$

where *f*, *I*, and θ are the wave frequency, inclination angle of the geomagnetic field, and elevation angle of the radio path, respectively. Letting $I = 49°$ and $B = 46{,}000$ nT, we obtain the parameters for the receivers at ORI (distance = 120 km, $\theta = 78.2°$) and SGD (distance = 146 km, $\theta = 75.7°$) as below.

$$\begin{aligned}
&(1)\ \text{ORI}\\
&f = 5\ [\text{MHz}] \quad V_{vert}[\text{m/s}] = -30.6\ \Delta f[\text{Hz}] \quad E[\text{mV/m}] = -2.15\ \Delta f[\text{Hz}]\\
&f = 8\ [\text{MHz}] \quad V_{vert}[\text{m/s}] = -19.2\ \Delta f[\text{Hz}] \quad E[\text{mV/m}] = -1.34\ \Delta f[\text{Hz}]\\
&(2)\ \text{SGD}\\
&f = 5\ [\text{MHz}] \quad V_{vert}[\text{m/s}] = -31.0\ \Delta f[\text{Hz}] \quad E[\text{mV/m}] = -2.17\ \Delta f[\text{Hz}]\\
&f = 8\ [\text{MHz}] \quad V_{vert}[\text{m/s}] = -19.3\ \Delta f[\text{Hz}] \quad E[\text{mV/m}] = -1.36\ \Delta f[\text{Hz}]
\end{aligned} \tag{3}$$

We used magnetometer data from Kakioka (KAK) at midlatitude, Kanoya (KNY) and Okinawa (OKI) at low latitude, and Yap (YAP) at the geomagnetic equator in the western Pacific zone and from Santa Maria (SMA) and Sao Luiz (SLZ) at low latitudes in Brazil (Table 1). We analyzed four SC events that occurred when the western Pacific was on the dayside, while Brazil was located on the nightside, The KAK, KNY, and OKI are supposed to be affected by the compressional waves, while YAP is affected by both the compressional wave and ionospheric currents intensified by the Cowling effect. So the difference between YAP and OKI or KNY is caused by the equatorial electrojet (hereafter denoted as EEJ). As shown below, the correlation between the HFD and EEJ will be a key to confirm that the electric field is the potential field associated with the ionospheric currents. The Brazilian stations provide information about the compressional wave propagating to the nightside.

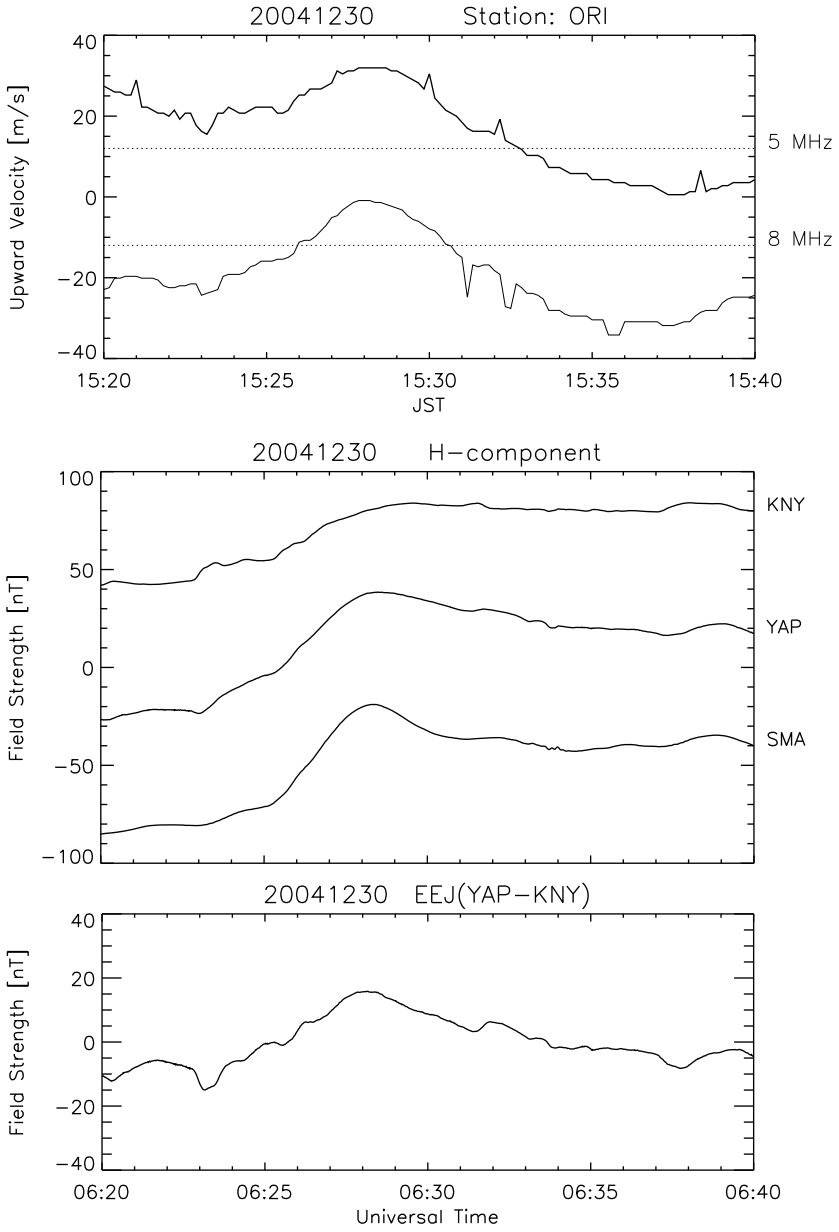

Figure 2. (top) Vertical motion of the ionosphere as observed with the HF Doppler sounder as a function of the Japan standard time (JST), (middle) H component magnetic fields at Kanoya (KNY), Yap (YAP), and Santa Maria (SMA), and (bottom) the equatorial electrojet (EEJ) obtained as a difference between YAP and KNY plotted in universal time (UT) for the SC event 1. The ionosphere in the afternoon moves upward during the MI and the motion is well correlated with the EEJ.

We also analyzed three more SC events to revisit the evening anomaly of the SCFs reported by *Kikuchi et al.* [1985], which will be an important feature to identify the electric field as the potential field.

The transmission of the ionospheric electric field and currents of the PI to the equator has been shown to be instantaneous with the temporal resolution of 10 s on both the dayside [*Araki*, 1977] and nightside [*Kikuchi*, 1986]. The TM_0 (TEM) mode wave carrying the electric field and currents has no low cutoff frequency [*Budden*, 1961] and does not suffer significant attenuation due to the finite ionospheric conductivity, but does suffer severe geometrical attenuation at the low latitude due to the finite size of the polar electric field [*Kikuchi et al.*, 1978; *Kikuchi and Araki*, 1979b]. The geometrical attenuation causes the transmitted electric field to be less than 10% of the polar electric field, but it is well recognized as the SCFs at middle and low latitudes and PI and MI at the geomagnetic equator.

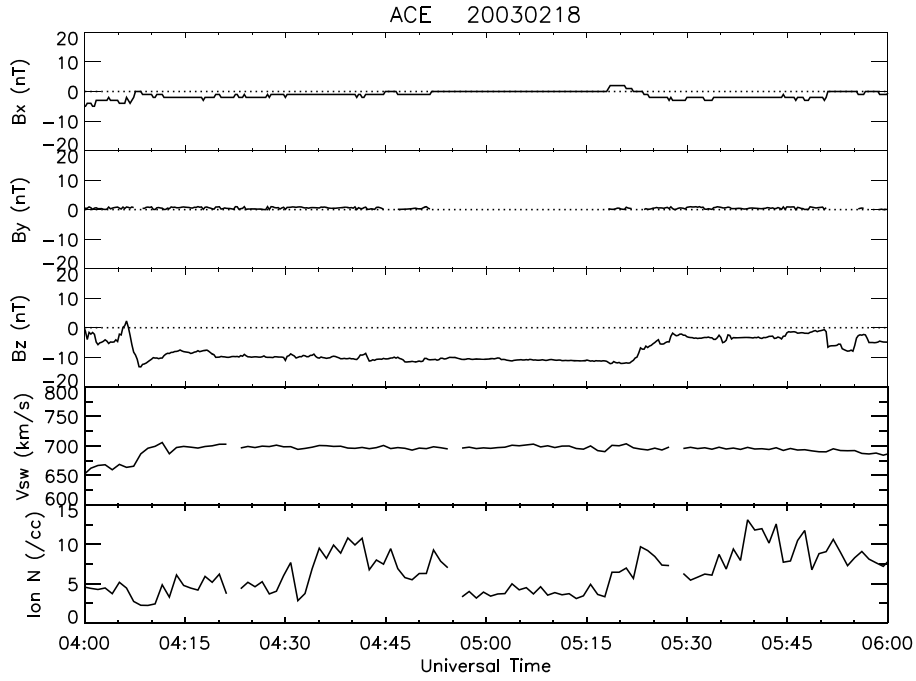

Figure 3. Solar wind parameters same as in Figure 1 for the SC event 2 on 18 February 2003. The increase followed by the decrease at around 0430 UT caused the compression and rarefaction effects on the H component on the ground.

2.2. SC Event 1

Figure 1 shows the solar wind magnetic fields (B_x, B_y, B_z), velocity (V_{sw}), and density (Ion N) detected by ACE (Advanced Composition Explorer) at the L-1 point for the SC event 1 on 30 December 2004. The solar wind density increased abruptly at 0535 UT by 30/cm^3 and no significant change from 500 km/s in the solar wind velocity. The sudden increase in the solar wind density caused the SC to be recorded at the low latitude (KNY) and equator (YAP) on the dayside (1530 LT) and at the low latitude (SMA) on the nightside (0230 LT) as shown in Figure 2 (middle). The SC started at 0623 UT simultaneously on the dayside and nightside and developed rather gradually with the peak at 0629 UT at KNY and at 0628 UT at YAP and SMA. The gradual increase at KNY indicates that the compressional waves continued to be arriving for 5 min during the MI of SC. It is noted that the SCs at YAP and SMA are similar to each other with the peak amplitude larger than that at KNY, which manifests the equatorial enhancement of SC at the dayside equator (YAP) and field-aligned current effects on the nightside (SMA) [*Araki et al*., 2006; *Shinbori et al*., 2009]. The PI at YAP is appreciable, but it is so short (<1 min) that the compressional effects cause the MI to predominate over the whole period of the SC.

Figure 2 (top) shows the vertical velocity of the ionosphere observed by the HF Doppler sounder at ORI with frequencies of 5 and 8 MHz as a function of local time (JST: Japan Standard Time). The velocity started to increase at the same time as the onset of the SC, reached the peak at 0628 UT (1528 JST) at the same time as the SC at YAP, and recovered gradually for 10 min. The plots for 5 and 8 MHz are almost identical except that the magnitude is a little larger at higher frequency, which means that the HFD is caused by changes in the reflection height rather than changes in the refractive index of the ionosphere below the reflection height [*Davies et al*., 1962]. The upward velocity of the ionosphere is preceded by a small downward velocity with the duration <1 min, but it is small and too short to represent the major ionospheric response to the compression of the magnetosphere continuing for over 10 min. It is remarkable that the upward motion of the dayside ionosphere is in opposite direction to what one might expect. The results suggest that the ionosphere is not compressed by the compressional waves, while the increase in the magnetic field arrives at the ground. The electric field responsible for the upward motion should not be the wave electric field but must be a potential field associated with the ionospheric currents [*Kikuchi et al*., 1985].

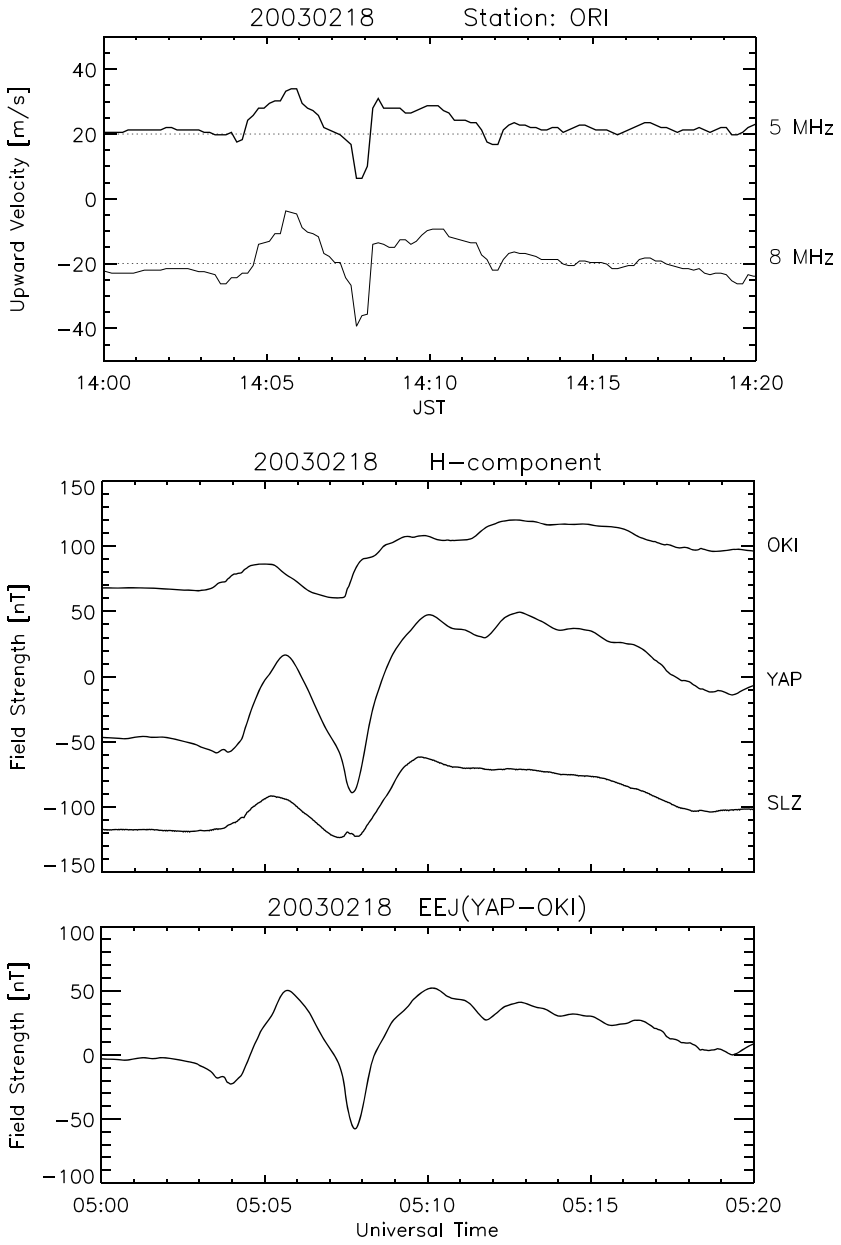

Figure 4. (top) Vertical motion of the ionosphere as observed with the HF Doppler sounder, (middle) H component magnetic fields at Okinawa (OKI), YAP, and Sao Luiz (SLZ), and (bottom) the EEJ derived from YAP and OKI for the SC event 2. The ionosphere moves upward/downward during the positive/negative MI and the motions are well correlated with the positive/negative EEJ.

To confirm the electric field being associated with the ionospheric currents, we plot the EEJ in Figure 2 (bottom), which is derived as the difference between the SCs at YAP and KNY. The vertical velocities are well correlated with the EEJ in all respects including the onset and peak times and duration times of the PI and MI. In particular, the initial downward motion exactly corresponds to the PI of the EEJ, indicating that the downward motion is caused by the dusk-to-dawn potential electric field of the PI [*Kikuchi*, 1986]. Thus, it is suggested that the electric field responsible for the ionospheric motion has been transmitted with the ionospheric currents from the polar ionosphere, matching the near-instantaneous transmission of the electric field and currents by the TM_0 mode electromagnetic waves in the Earth-ionosphere waveguide [*Kikuchi et al.*, 1978; *Kikuchi and Araki*, 1979b].

2.3. SC Event 2

Figure 3 shows the solar wind magnetic fields (B_x, B_y, B_z), velocity (V_{sw}), and density (Ion N) for the SC event 2 on 18 February 2003 in the same format as in Figure 1. The solar wind density increased at 0430 UT followed by an impulsive decrease during the period of constant negative B_z (10 nT) and constant velocity (700 km/s). The impulsive fluctuations in the solar wind density would cause a sequence of compression and rarefaction of the magnetosphere, resulting in the SC fluctuating rather than stepwise as shown in Figure 4 (middle). The SC at YAP peaked with a delay from those at OKI and SLZ by about 1 min and is preceded by a negative deflection with 1 min duration. Similarly to the SC event 1, the SC at YAP is larger than that at OKI due to the superposition of the EEJ on the DL.

Figure 4 (top) shows the vertical velocity observed by the HF Doppler sounder at ORI, composed of upward, downward, and upward motions corresponding to the series of compression and rarefaction of the magnetosphere, although the upward/downward motion is slightly delayed from the compression/rarefaction effects at OKI. One may notice that a small magnitude downward motion occurred at 0503 UT (1403 JST) on the 8 MHz curve. This downward motion occurred at the same time as the arrival of the SC at OKI, but the motion of the ionosphere turns upward at 0505 UT when the compressional effects attained the peak at OKI. Likewise, the sharp downward motion at 0508 UT corresponds to the increase in the DL at OKI, but we note that it exactly corresponds to the sharp decrease at YAP, indicating the westward electric field associated with the negative EEJ. To verify the downward/upward motion of the ionosphere being caused by the dusk-to-dawn/dawn-to-dusk potential field, we show the EEJ in Figure 4 (bottom). The vertical velocity perfectly coincides with the EEJ in all respects, in particular, the downward motions at 0504 UT and 0508 UT correspond to the negative EEJ. We thus confirmed that the ionosphere moves upward/downward when the magnetosphere is compressed/rarefied, which is caused by the dawn-to-dusk/dusk-to-dawn potential electric field associated with the ionospheric currents.

2.4. SC Event 3

Figure 5 (top) shows the velocity of the motion of the ionosphere, SCs recorded at OKI, YAP, and SMA (Figure 5, middle), and EEJ derived from the SCs at YAP and OKI (Figure 5, bottom) in the same format as in Figures 2 and 4. The stepwise increase in the H component started at 2242 UT at OKI caused by an abrupt increase in the solar wind density at 2210 UT (data not shown), followed by some quasiperiodic fluctuations and ended with the stepwise decrease at 2251 UT. Unlike the previous events, the stepwise increase is not amplified at YAP for the first 3 min after the onset (2242–2245 UT). This feature indicates that the beginning part of the SC is caused only by the magnetopause currents without contribution of ionospheric currents. In contrast, the latter part of the SC over the period 2245–2251 UT is amplified at YAP and, furthermore, the sharp decrease at 2251 UT is also amplified with a time delay of 1 min. Although the reason is not clear, the unexpected behavior of the ionosphere over the first 3 min clearly indicates no response of the ionosphere to the compressional wave but shows incompressible nature of the ionosphere. In contrast, the ionosphere moved upward during the latter 6 min due to the eastward electric field corresponding to the equatorial enhancement of the SC. Figure 5 (bottom) shows that the EEJ started to develop at 2245 UT when the ionosphere started to move upward. It is suggested again that the ionospheric motion is caused by the electric field transmitted together with the ionospheric currents from the polar ionosphere. It is to be noted that short-period (2 min) fluctuations are superimposed on the SC. These fluctuations might have been carried by the compressional waves as observed at OKI. Interestingly, however, the fluctuations are also observed in the vertical motion and EEJ with excellent correlations. These results suggest that ULF range fluctuations in the ionospheric currents extend to the equator and the electric field associated with the currents drives the oscillating motion of the ionosphere similar to the global PC5 events [*Motoba et al*., 2002].

2.5. SC Event 4

Figure 6 (top) shows the velocity of the motion of the ionosphere, SCs recorded at OKI, YAP, and SLZ (Figure 6, middle), and EEJ derived from the SCs at YAP and OKI (Figure 6, bottom) in the same format as in the previous events. The SC began at 0611:30 s UT on 29 October 2003 and the amplitude is 70 nT at OKI and 120 nT at YAP showing the contribution of the EEJ at YAP. It is to be noted that no PI precedes the SC at YAP in contrast to the previous events and that the SC is characterized by the short rise time of about 20 s at OKI. Another remarkable feature of the SC is superposition of 1 min period oscillations with some time delay (10–20 s) at YAP from OKI. On the other hand, the vertical motion of the

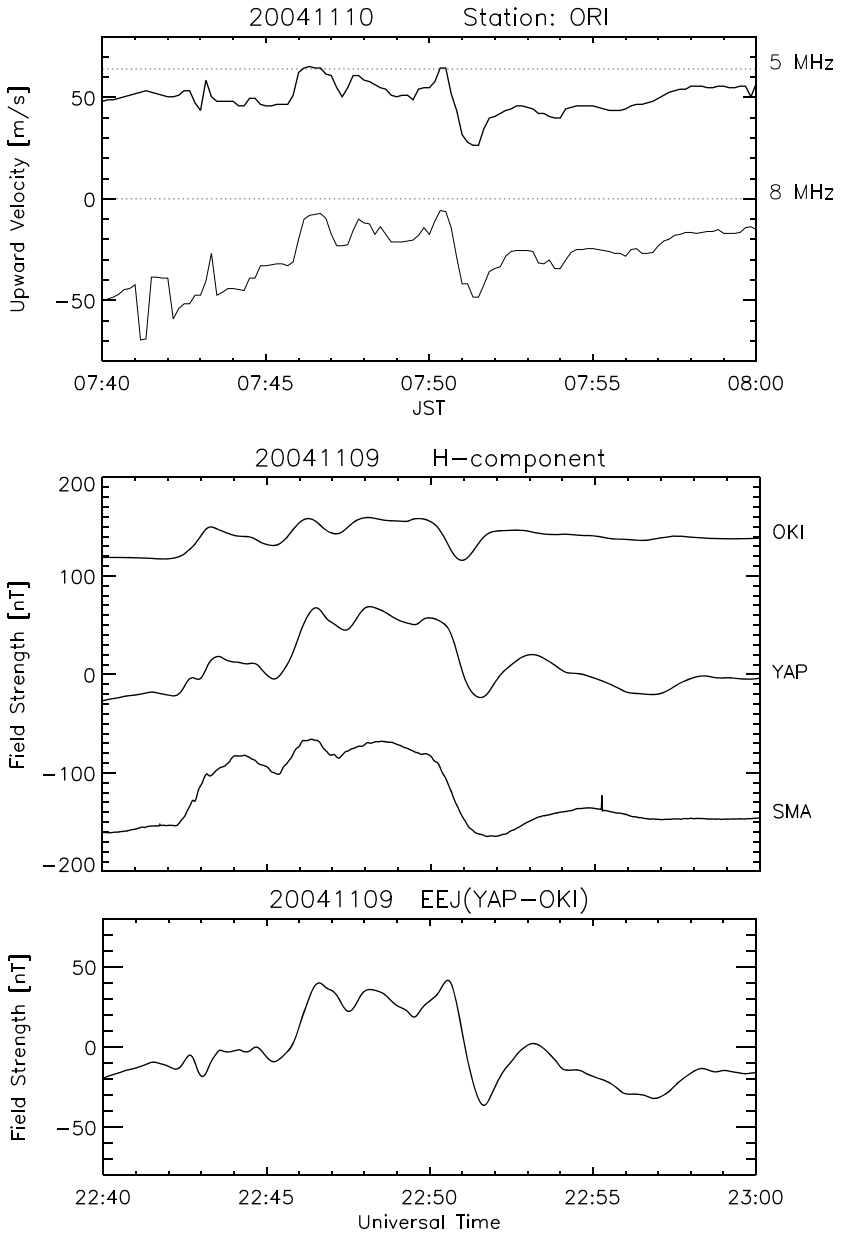

Figure 5. (top) Vertical motion of the ionosphere as observed with the HF Doppler sounder, (middle) H component magnetic fields at OKI, YAP, and SMA, and (bottom) the EEJ for the SC event 3 on 9 November 2004. The ionosphere does not move during the first 3 min of the MI, while it moves upward during the latter 5 min. The motion of the ionosphere is well correlated with the EEJ.

ionosphere started with an impulsive downward motion followed by the upward motion superimposed on the 1 min period oscillations (Figure 6, top). The initial downward motion occurred at the onset of the SC at OKI, which might be considered to be evidence for a possible compressional motion by the compressional wave. However, the EEJ is found to begin with the negative PI for 20 s as shown in Figure 6 (bottom), which exactly corresponds to the impulsive downward motion. No appearance of the PI at YAP may be due to faster development of the DL than the PI. In other words, the compressional waves arrived at the low-latitude ionosphere before the PI currents arrived at the equatorial ionosphere, simply because the magnetopause currents were located much closer to the Earth than in the normal SC events as inferred from the anomalously short rise time (20 s). Consequently, the vertical velocity absolutely matches the EEJ during the PI and MI and also during the oscillations.

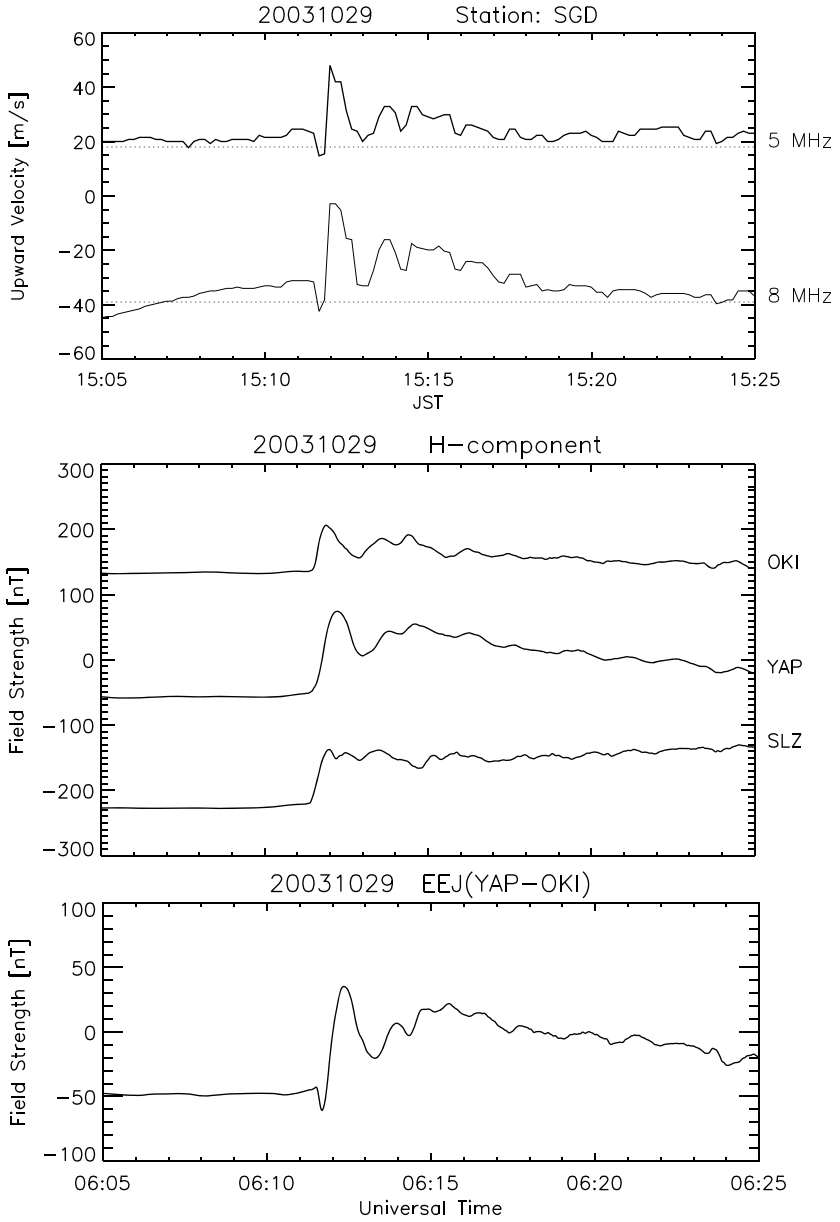

Figure 6. (top) Vertical motion of the ionosphere as observed with the HF Doppler sounder, (middle) H component magnetic fields at OKI, YAP, and SLZ, and the EEJ for (bottom) the SC event 4 on 29 October 2003. The ionosphere moves downward at the beginning of the MI while it moves upward during the whole period of the MI and is well correlated with the EEJ. The initial downward motion is well correlated with the negative EEJ of the PI of SC.

2.6. FAC Signatures in the Equivalent Currents at High Latitudes

The above results suggest that the electric field in the midlatitude *F* region ionosphere is westward during the PI and eastward during the MI, which are a dayside part of the dusk-to-dawn and dawn-to-dusk potential electric fields transmitted from the polar ionosphere together with the ionospheric currents. During the PI of SC, the electric potentials and a pair of FACs are generated by the localized compression of the magnetopause, propagating down the magnetic field lines with the transverse wave (Alfven wave) [*Tamao*, 1964]. One minute later, another pair of FACs is generated inside the magnetosphere so as to enhance the convection electric field [*Araki*, 1994], providing the dawn-to-dusk potential electric field to the polar ionosphere. The electric potentials propagate to low latitudes at the speed of light with the TM_0 (TEM) mode waves in the Earth-ionosphere waveguide [*Kikuchi et al.*, 1978; *Kikuchi and Araki*, 1979b], achieving the quasi-steady Pedersen current circuit down to the equator with time constants of a few to 10 s [*Kikuchi*, 2014].

In the high-latitude ionosphere, the electric fields drive the Hall current vortices encircling the FACs clockwise in the morning and anticlockwise in the afternoon during the PI and vice versa during the MI. The Hall currents can be observed as the equivalent currents deduced from the ground magnetometer network data. Y. Nishimura et al. (Evolution of the current system during solar wind pressure pulses based on aurora and magnetometer observations, under review, 2016), using SuperMAG [*Gjerloev*, 2012] magnetometer data in the Northern Hemisphere and DMSP magnetometer and particle data as well as the optical aurora, confirmed that the equivalent current vortices are associated with the field-aligned currents of the PI and MI.

Figure 7 shows vector maps of the equivalent currents in the Northern Hemisphere during the SC event 1, where the noon is to the top (red line) and the midnight to the bottom (blue line). Before the onset of the SC, the clockwise current shear has developed in the morning sector (red arrows in Figure 7a1), which should be associated with the downward Region 1 field-aligned current. The current vortex then changes to the counterclockwise at 0623-0624 UT during the PI (Figures 7a2 and 7a3), indicating the upward FAC in the morning sector. It is to be noted that the PI FAC remains at 0624 UT when the electric field of the PI has decayed at midlatitudes (Figure 2). This is because the midlatitude electric field is a superposition of the PI and newly born MI electric fields. After the transition (Figure 7a4), the current vortex becomes clockwise in the morning sector (Figures 7b5–7b7), which encircles the downward FAC of the MI. The concurrent development of the ionospheric currents at the high latitude and equator and of the electric field at midlatitudes supports our scenario that the electric field is transmitted from the polar ionosphere to the midequatorial latitudes together with the ionospheric currents.

3. Evening Anomaly of the Midlatitude Electric Fields

Kikuchi et al. [1985] showed that the SCF is (+ −) in the day and evening hours, while (− +) in the night. The PFD and MFD are primarily caused by the dusk-to-dawn and dawn-to-dusk potential fields, respectively, but the daytime SCF pattern extends to the evening hours (1800–2200 LT). *Tsunomura* [1999], using the potential solver with an input of the field-aligned currents in the polar ionosphere, suggested that the evening anomaly is derived from the asymmetric distribution of the electric potential in the global ionosphere with the Hall effects and the day-night inhomogeneity of the conductivities. Indeed, model calculations by *Nopper and Carovillano* [1978] and *Senior and Blanc* [1984] also show similar evening anomalies of the electric fields. All these model calculations also predict that the electric field is enhanced significantly in the evening compared with that in the day. In this section, we examine if the PI and MI electric fields are enhanced in the evening by analyzing three SC events. We further confirm that the evening enhancement is due to the global distribution of the electric potential by reproducing the PI and MI electric fields with the global MHD simulation [*Tanaka*, 2007] that employs the potential solver at the inner boundary of the magnetosphere-ionosphere coupling.

Figure 8 (top) shows the SCF (+ −) in the day (1650 LT) and evening (1955 LT) (Figure 8, middle) and SCF (− +) in the night (0040 LT) (Figure 8, bottom), representing the local time features of the SCF reported by *Kikuchi et al*. [1985]. It is commonly observed in the three events that the duration times of the PFD and MFD are approximately 1 and 5 min, respectively. To show the evening enhancement of the PI and MI electric fields, we compare the electric fields deduced from the SCF with the EEJ as well as the *SYM-H*. Figure 9 (row 1) shows the electric field, EEJ in the same local time as for the SCF (Figure 9, row 2), EEJ in the daytime derived from the African equatorial (AAE) and low latitude (TAM) stations (Figure 9, row 3) and *SYM-H* (Figure 9, row 4) for the SC events in the day (Figure 9, left column) and evening (Figure 9, right column). It is observed that the peak-to-peak magnitude of the electric field is 3.5 mV/m in the day and 11 mV/m in the evening. It is remarkable that the evening time electric field is 3 times stronger than that in the day, in spite of the larger amplitude of the *SYM-H* and EEJ in the daytime event. This local time feature indicates the evening enhancement of the PI and MI electric fields. It is to be noted that the evening time electric fields are so strong as to drive the EEJ at YAP where the ionosphere is absolutely in the dark.

To confirm that the PI and MI electric fields are potential fields and that the evening anomaly is due to the asymmetric distribution of the electric potential in the global ionosphere, we reproduced the PI and MI electric fields with the global MHD simulation of *Tanaka* [1995, 2007] that employs the potential solver at the inner boundary of the M-I coupling. Figure 10 shows sequence of the PI and MI electric fields reproduced for the day (Figure 10, top), evening (Figure 10, middle), and night (Figure 10, bottom) at the midlatitude (25° geomagnetic latitude).

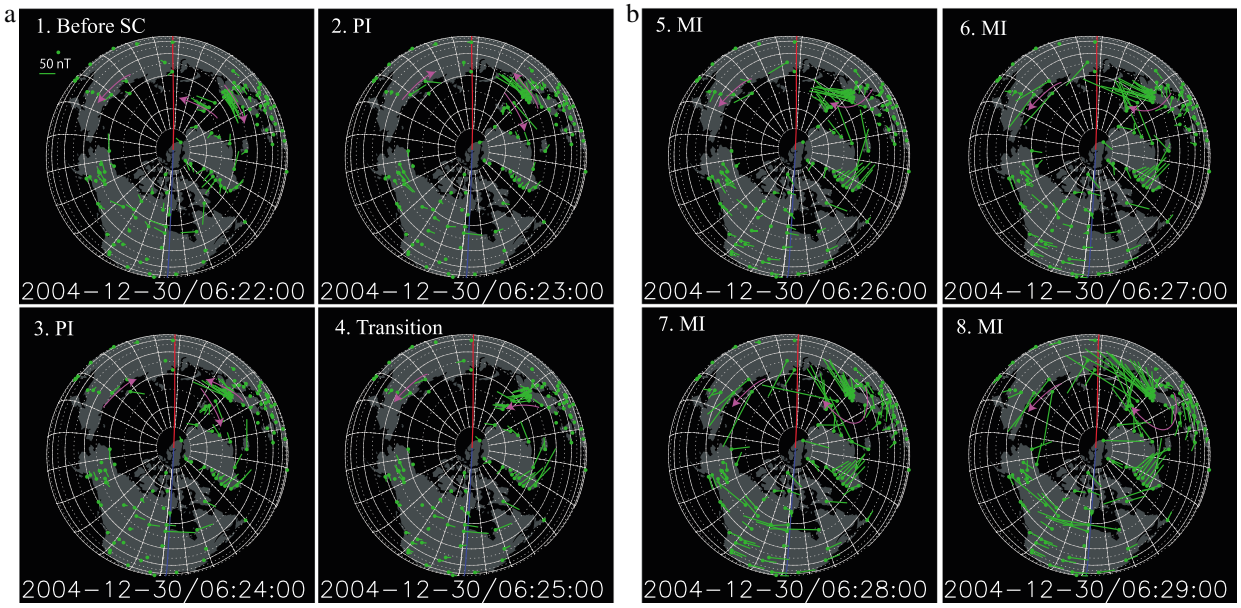

Figure 7. (a, b) Equivalent current vectors derived from the ground magnetometer network for the periods (1) before SC and (2, 3) during the PI, (4) transition, and (5–8) MI periods for the SC event 1. The noon is to the top (red line) and the midnight to the bottom (blue line). The clockwise vortex shown with the red arrows in the morning sector (Figures 7a2 and 7a3) is related to the upward field-aligned current of the PI and the clockwise vortex (Figures 7b5–7b8) in the morning sector is related to the downward FAC of the MI.

The duration of the PI and MI electric fields are 1–2 min and >5 min, respectively, and the magnitude of the MI electric field is greater than that of the PI. Furthermore, the evening time electric fields are in the same polarity as in the daytime with significant enhancement of the magnitude. The simulation results are remarkably similar to the observations in all respects. In particular, the evening anomaly is reproduced by solving the Poisson equation for the electric potential. We conclude that the PI and MI electric fields are potential fields transmitted with the ionospheric currents from the polar ionosphere which have been supplied by the field-aligned currents.

4. Discussion

When the solar wind shock hits the magnetosphere, the magnetopause currents are intensified and launch an increase in the magnetic field that will be observed as the SC at low latitude (DL of SC [*Araki*, 1977]). According to *Tamao*'s [1964] theory, the propagation of the launched waves is described by the following equation (the SI unit is used below):

$$\nabla^2 A - \frac{1}{V_A{}^2}\frac{\partial^2 A}{\partial t^2} = -\frac{\mu_0}{B^2} F \times B, \tag{4}$$

where ***A, F, B,*** and V_A denote the magnetic vector potential, external force exerted on the magnetopause, ambient geomagnetic field, and Alfven speed, respectively, and μ_0 is the magnetic permeability. Two modes are excited by the external force, and their propagation is described by the following equations as quoted from Tamao's equations (2.6) and (2.7),

$$\left(\frac{\partial^2}{\partial z^2} - \frac{1}{V_A{}^2}\frac{\partial^2}{\partial t^2}\right)\nabla \cdot A_\perp = -\frac{\mu_0}{B^2}\nabla \cdot (F \times B) \tag{5}$$

$$\left(\nabla^2 - \frac{1}{V_A{}^2}\frac{\partial^2}{\partial t^2}\right)\nabla_z \times A_\perp = -\frac{\mu_0}{B^2}\nabla_z \times (F \times B) \tag{6}$$

The $\mathrm{div} A_\perp$ is communicated one dimensionally along the magnetic field lines (z axis) through the source, while $\mathrm{rot}_z A_\perp$ spreads in all directions from the source. These waves are referred to as the transverse (Alfven) and isotropic (compressional) waves, respectively [*Tamao*, 1964].

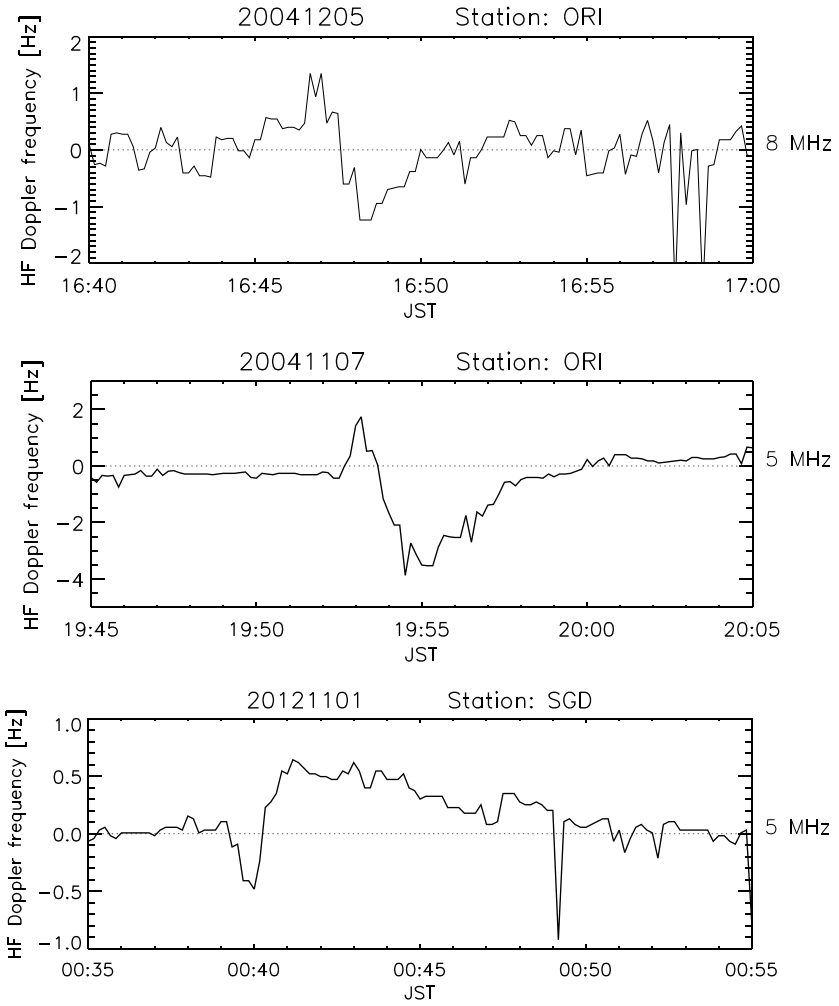

Figure 8. SCFs recorded as a function of the local time (JST) during separate geomagnetic sudden commencements, representing the (top) SCF (+ −) in the day, (middle) SCF (+ −) in the evening, and (bottom) SCF (− +) in the night. The SCF comprises the preliminary frequency deviation (1 min) followed by the main frequency deviation (>5 min).

The compressional wave is alternatively expressed by the following equation (Tamao's (3.1)),

$$\left(\nabla^2 - \frac{1}{V_A{}^2}\frac{\partial^2}{\partial t^2}\right) h_z = \frac{\mu_0}{B^2} B\nabla\cdot F_\perp, \tag{7}$$

where h_z is the increase in the magnetic field parallel to $\boldsymbol{B}$ and the right-hand side represents the compression of the magnetopause toward the Earth. The compressional wave propagates across the magnetic field lines in the magnetosphere on both the dayside and nightside as observed on board spacecrafts [*Wilken et al*., 1982; *Shinbori et al*., 2004] to be observed on the ground as the DL of SC [*Araki*, 1994].

In the partially ionized *F* region ionosphere, the compressional wave suffers attenuation, although it is not severe propagating over a few hundreds of kilometers and then changes to the diffusion mode wave in the conducting *E* region ionosphere [*Kikuchi and Araki*, 1979a]. The electric field of the compressional wave is westward at all local times, driving the earthward motion of the magnetized plasma in the magnetosphere [*Shinbori et al*., 2004]. Therefore, one might expect that the ionosphere undergoes compression when the compressional wave arrives at the ionosphere. Indeed, there have been several theoretical models where the compression/rarefaction of the ionosphere plays a major role in creating the HF Doppler frequencies during the SC and ULF pulsations [*Jacobs and Watanabe*, 1963; *Poole et al*., 1988; *Sutcliffe and Poole*, 1990; *Pilipenko et al*., 2010]. Among others, the downward motion detected as the positive PFD was attributed to the electric field of the compressional wave [*Huang et al*., 1973; *Pilipenko et al*., 2010]. However, as shown in the present paper (events 1 and 2, Figures 2 and 4), the

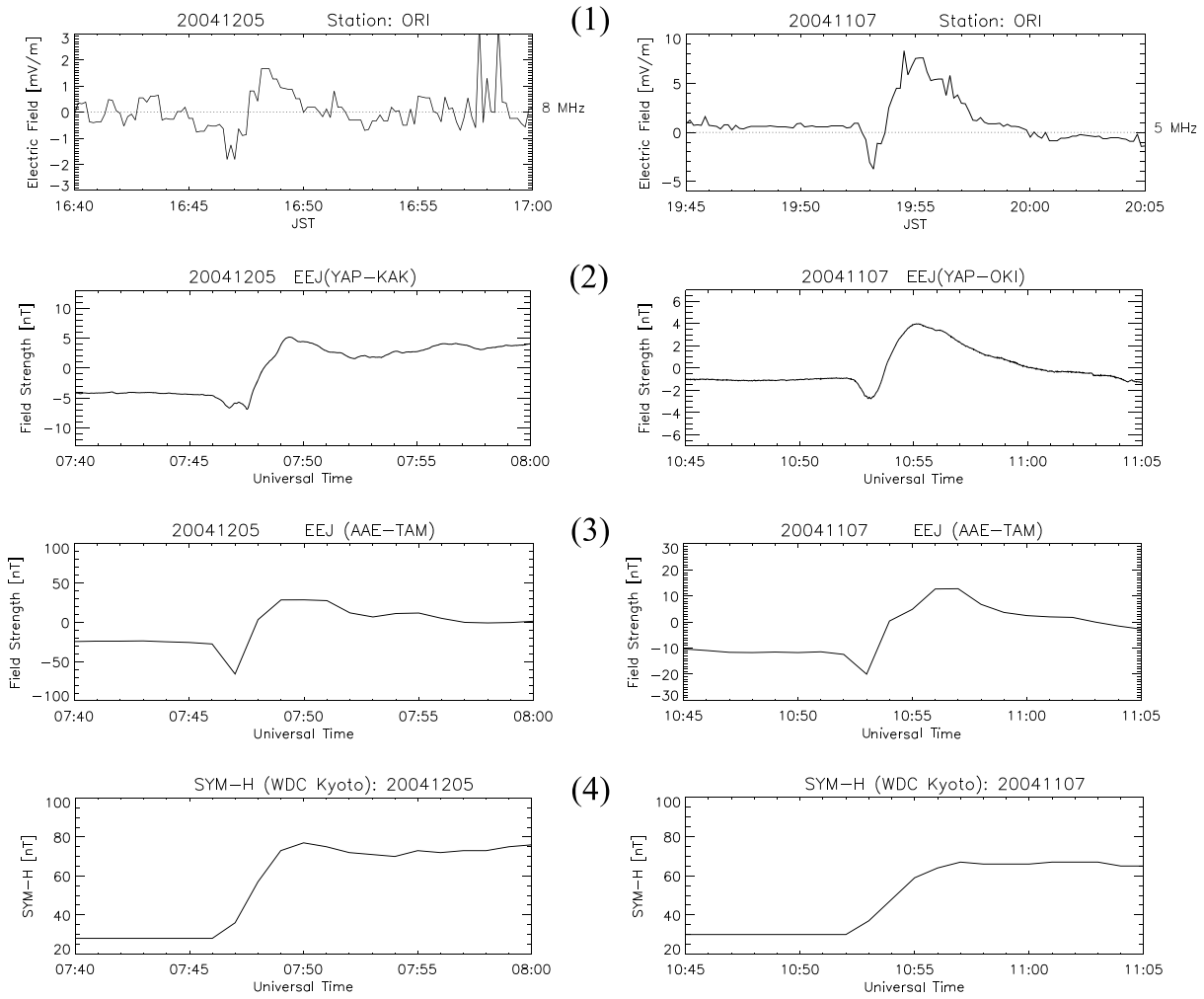

Figure 9. The electric field derived from the SCF (left column) in the afternoon and (right column) in the evening. (row 2) The EEJ at YAP in the same local time as for the SCF and (row 3) the EEJ in the daytime derived from AAE and TAM. (row 4) *SYM-H* to indicate the magnitude of the events. The electric field is 3 times stronger in the evening than in the afternoon, although the *SYM-H* is a bit smaller in the evening.

ionosphere never moves downward during the period of the magnetospheric compression, but instead moves upward due to the eastward potential electric field associated with the ionospheric currents. Furthermore, the SC event 3 (Figure 5) reveals no response of the ionosphere during the first 3 min of the compression of the magnetosphere. We do not have any convincing explanation for the inactive period, but the ionosphere is never compressed by the compressional waves and the following upward motion is perfectly correlated with the intensification of the equatorial electrojet (Figure 6). We have shown the other example of the downward motion of the ionosphere during the magnetospheric compression (Figure 7). Even in this event, the downward motion was found to correspond to the negative PI at the equator (Figure 8), suggesting again that the ionospheric motion is caused by the potential electric field associated with the ionospheric currents.

Here we examine how the ionosphere responds to the compressional wave. *Kikuchi and Araki* [1979a] studied the step response of the ionosphere by giving a stepwise increase in the magnetic field simulating the arrival of the SC. It was shown that the *F* region ionosphere nearly behaves as the MHD medium, while the *E* region behaves as the conductor as studied by *Watanabe* [1962], in which the propagation is described by the diffusion equation as below.

$$\frac{\partial B_x}{\partial t} - \frac{1}{\mu_0 \sigma}\frac{\partial^2 B_x}{\partial z^2} = 0, \tag{8}$$

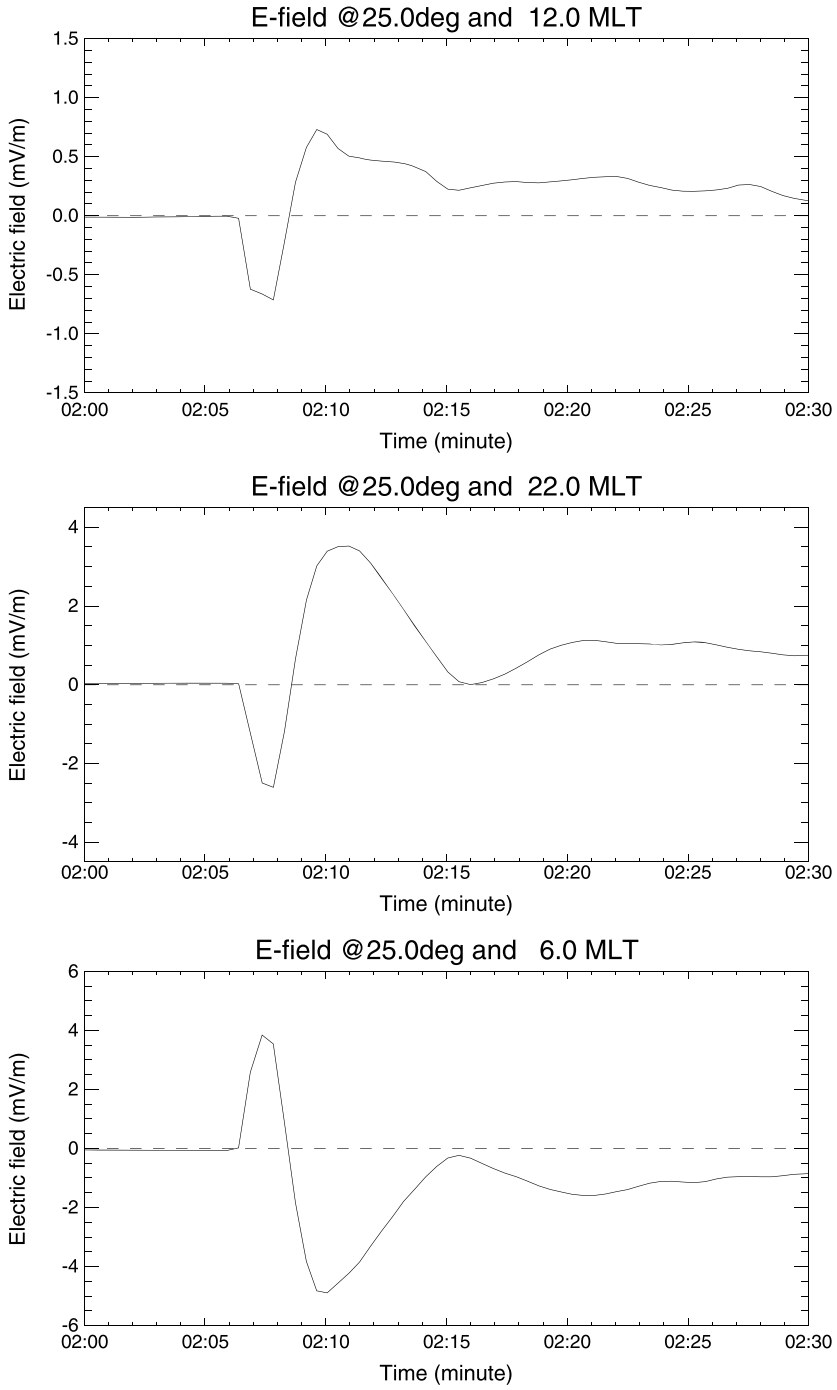

Figure 10. The PI and MI electric fields reproduced by the global MHD simulations for the (top) day, (middle) evening, and (bottom) night. The reproduced PI and MI electric fields have the time scale of 1–2 and >5 min, respectively and show the evening anomaly with the polarities same as in the day and enhanced magnitude.

where σ (mho/m) denotes the conductivity of the conducting ionosphere and the coordinates, x (northward), y (eastward), and z (downward) are employed. To simulate the SC event 1 with the rise time of 5 min, we assume that the incident B_x varies in the form (9) below, which increases straight to the constant value, B_0 as shown in Figure 11 (top left):

$$B_x[t] = \frac{B_0}{t_0}\{t \cdot U[t] - (t - t_0)U[t - t_0]\}, \tag{9}$$

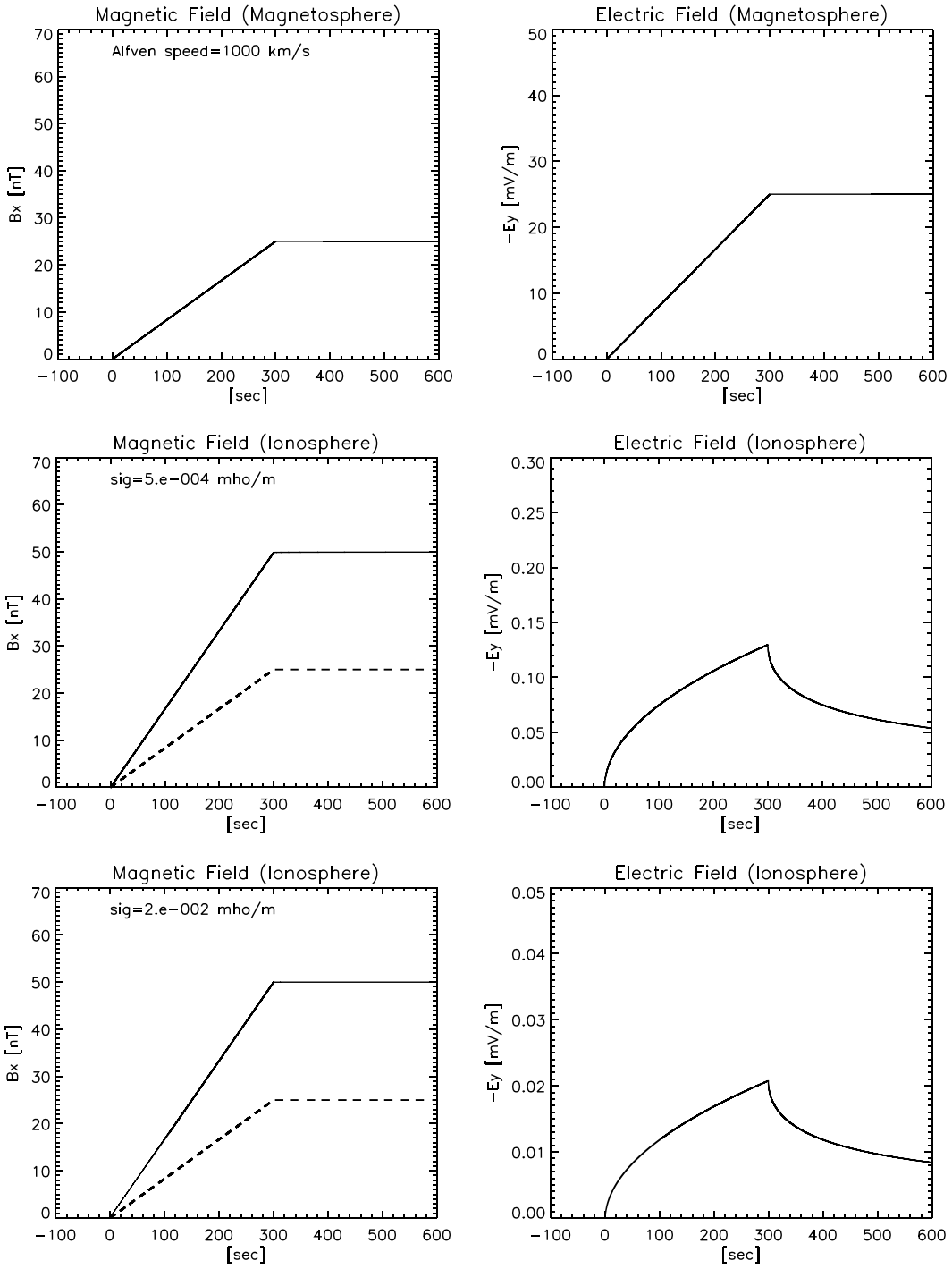

Figure 11. The (left column) magnetic and (right column) electric fields propagating one dimensionally in the (top row) uniform magnetosphere and at the surface of the conducting ionosphere with the conductivity of (middle row) $5 \cdot 10^{-4}$ mho/m, and (bottom row) $5 \cdot 10^{-2}$ mho/m. The magnetic field is doubled at the surface of the conducting ionosphere, while the electric field is severely suppressed to be less than 1/100 and 1/1000 of the incident wave for the two cases. The incident magnetic field is shown with the dashed curves in Figures 11 (middle row) and 11 (bottom row) as a reference.

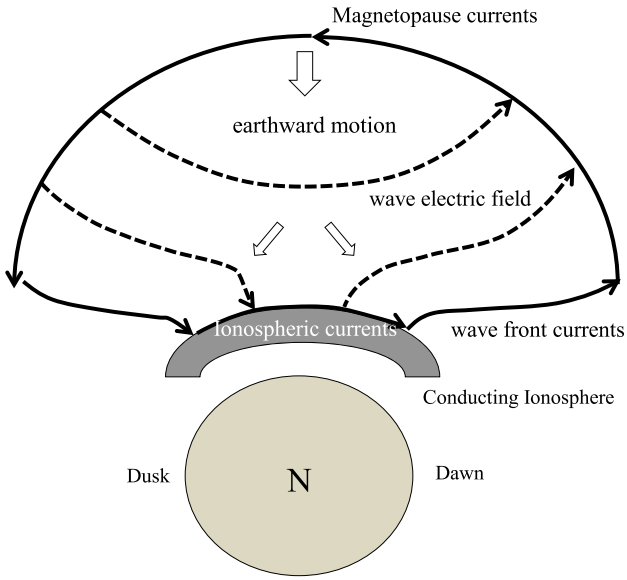

Figure 12. Schematic diagram of the current circuit in the equatorial plane that would be established when the compressional waves arrive at the conducting ionosphere. The solid curves indicate the electric currents closing from the magnetopause to the ionosphere via the polarization currents on the wave front of the compressional wave. The dashed curves indicate the electric field carried by the compressional waves which is perpendicular to the surface of the ionosphere as a result of the severe suppression of the tangential component. The motion of the plasma is indicated with the open arrows.

where $U(t)$ and t_0 denote the unit step function and rise time, respectively. We assume that B_0 of the incident wave is 25 nT. Then the electric field, E_y, in the magnetosphere is 25 mV/m provided that the Alfven speed is 1000 km/s (Figure 11, top right).

Equation (8) can be readily solved by employing the Laplace transformation. The B_x and E_y thus obtained are given with the complementary error function as below.

$$B_x = 2\frac{B_0}{t_0}\left(\begin{array}{l}\left(t+\frac{1}{2}z^2\mu_0\sigma-\frac{z}{V_A}\right)\mathrm{erfc}\left(\frac{z\sqrt{\mu_0\sigma}}{2\sqrt{t}}\right)U[t]-\left(z\sqrt{\mu_0\sigma}+\frac{2}{V_A\sqrt{\mu_0\sigma}}\right)\sqrt{\frac{t}{\pi}}e^{-\frac{z^2\mu_0\sigma}{4t}}U[t]\\ -\left(t-t_0+\frac{1}{2}z^2\mu_0\sigma-\frac{z}{V_A}\right)\mathrm{erfc}\left[\frac{z\sqrt{\mu_0\sigma}}{2\sqrt{t-t_0}}\right]U[t-t_0]\\ +\left(z\sqrt{\mu_0\sigma}+\frac{2}{V_A\sqrt{\mu_0\sigma}}\right)\sqrt{\frac{t-t_0}{\pi}}e^{-\frac{z^2\mu_0\sigma}{4(t-t_0)}}U[t-t_0]\end{array}\right) \tag{10}$$

$$E_y = -2\frac{B_0}{t_0}\frac{1}{\sqrt{\mu_0\sigma}}\left(\begin{array}{l}\left(z\sqrt{\mu_0\sigma}-\frac{1}{V_A\sqrt{\mu_0\sigma}}\right)\mathrm{erfc}\left[\frac{z\sqrt{\mu_0\sigma}}{2\sqrt{t}}\right]U[t]+2\sqrt{\frac{t}{\pi}}e^{-\frac{z^2\mu_0\sigma}{4t}}U[t]\\ -\left(z\sqrt{\mu_0\sigma}-\frac{1}{V_A\sqrt{\mu_0\sigma}}\right)\mathrm{erfc}\left(\frac{z\sqrt{\mu_0\sigma}}{2\sqrt{t-t_0}}\right)U[t-t_0]\\ -2\sqrt{\frac{t-t_0}{\pi}}e^{-\frac{z^2\mu_0\sigma}{4(t-t_0)}}U[t-t_0]\end{array}\right) \tag{11}$$

The B_x and E_y obtained with $5 \cdot 10^{-4}$ (mho/m) for σ are plotted with the solid lines in Figure 11 (middle row), along with B_x in the magnetosphere with the dashed lines as a reference. In Figure 11 (bottom row) are plotted the B_x and E_y with $5 \cdot 10^{-2}$ (mho/m), which simulates the case where the E_y is affected by the perfectly conducting ground located 100 km below the ionosphere. It is observed that B_x is doubled at the surface of the E region ionosphere because of the reflection from the conductor, while the E_y is suppressed severely to become less than 1/100 and 1/1000 of the electric field of the compressional wave. Since the horizontal electric field is

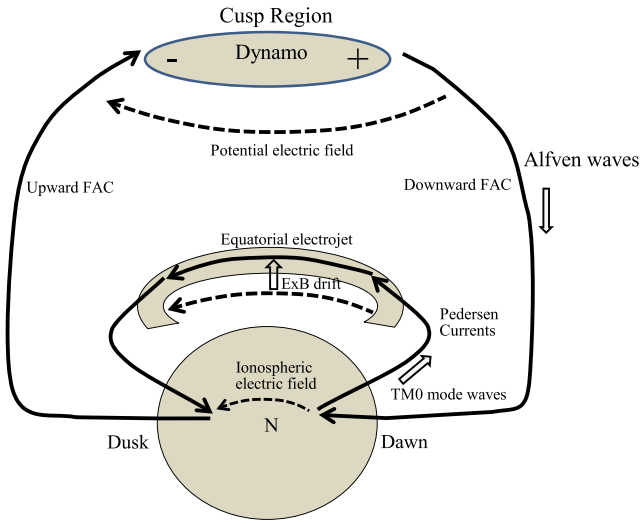

Figure 13. Schematic diagram of the current circuit established during the MI of SC between the magnetospheric dynamo and equatorial ionosphere via the polar ionosphere. The electric field and currents are transmitted by the Alfven waves accompanying field-aligned currents in the magnetosphere and by the TM_0 mode waves accompanying ionospheric currents to the equatorial ionosphere. The electric field in the ionospheric currents goes upward into the *F* region ionosphere driving the upward motion of the dayside midlatitude ionosphere correlated with the EEJ.

continuous on both sides of the interface between the conductor and MHD medium, the electric field in the *F* region should be about the same as plotted in Figure 11. Therefore, the compressional motion of the *F* region ionosphere would be severely damped. The B_x, on the other hand, diffuses into the ionosphere to be observed on the ground with time lag of a few seconds [*Kikuchi and Araki*, 1979a].

In the realistic model, we need to consider the effects of the almost perfectly conducting ground/sea where the horizontal electric field is zero. *Greifinger and Greifinger* [1968] showed that the boundary condition at the ground makes serious effects on the wave propagation in the *F* region ionosphere where the compressional waves propagate horizontally carrying the Pc1 pulsations to lower latitudes. The *F* region ionosphere forms a waveguide centered at the F_2 ionization peak, but the waves with frequency lower than the cutoff frequency of 0.5 Hz suffer severe attenuation due to the boundary condition at the ground. The theoretical model tells us that the compressional waves are severely attenuated in the *F* region ionosphere even for downward propagation. Actually, *Kivelson and Southwood* [1988] discussed that the electric field of the fast mode waves (compressional wave) should be zero for the ULF waves with frequencies <10 mHz. They explained that the fast mode wave is perfectly reflected at the ionosphere, based on the relations between the magnetic field and electric field under strong effects of the perfectly conducting ground.

Figure 12 shows a schematic diagram of the electric field (dashed curves) and currents (solid curves) that would be established at the moment when the compressional waves arrive at the conducting ionosphere. The ionospheric currents are to be connected with the polarization currents flowing on the wave front of the compressional wave as if the magnetized plasma behaves as the dielectric medium with the permittivity, $\varepsilon = \frac{\rho}{B^2}$ where ρ is the mass density of the plasma [*Spitzer*, 1962]. Consequently, it would be reasonable to draw the electric field lines perpendicular to the ionosphere in a similar way to those around the conductor embedded in the dielectric medium (Figure 12).

It should be recalled that both the PI and MI electric fields are in opposite direction on the dayside to nightside except in the evening hours. The electric field should have convergence/divergence around the terminators and should be connected with the Pedersen currents at midlatitudes and further to the field-aligned currents in the polar ionosphere. The ionospheric current vortex in Figure 7 assures development of the field-aligned currents in the polar ionosphere. It should be noted that the PI and MI electric fields show the strong local time asymmetry with the evening anomaly (Figures 8 and 9). Based on the potential solver results, *Tsunomura* [1999] pointed out that the evening anomaly should be derived from the asymmetric distribution of the electric potentials caused by the Hall effects and the day-night inhomogeneity of the ionospheric conductivity. The MHD simulations employing the potential solver at the inner boundary of the M-I coupling successfully reproduced the evening anomaly of the PI and MI electric fields as shown in Figure 10. The evening anomaly is such a unique feature of the electric potentials that its presence would help distinguish the potential fields from the wave fields.

Tamao [1964] showed that the electric potential and FACs of the PI are generated by the divergence of the magnetopause currents as described by (5). According to the global MHD simulation [*Slinker et al.*, 1999; *Fujita et al.*, 2003a], on the other hand, the FACs of the PI are generated off the magnetopause. One might

expect that the FACs can be generated by the mode conversion from the compressional wave. Indeed, *Tamao* [1964] suggested that the mode conversion occurs as expressed by the second term of the following equation (Tamao's equation (3.2)), which is named the converted transverse mode.

$$\left(\frac{\partial^2}{\partial z^2}-\frac{1}{V^2}\frac{\partial^2}{\partial t^2}\right)A_\perp=-\frac{\mu_0}{B^2}F\times B+\nabla_\perp\times h_z \tag{12}$$

The second term of the right-hand side represents the polarization current on the wave front of the compressional wave, and its divergence should be zero. Thus, the mode conversion at the wave front never generates the FACs.

During the MI of SC, the magnetospheric convection is enhanced in the compressed magnetosphere and propagates to the polar ionosphere, providing the dawn-to-dusk electric field and FACs with the direction opposite to the PI currents [*Araki*, 1994]. The global MHD simulations have successfully reproduced the electric potentials and field-aligned currents [*Slinker et al*., 1999; *Fujita et al*., 2003a, 2003b; *Tanaka*, 2007] and the consecutive appearance of the PI and MI electric fields at midlatitudes with duration times of 1–2 min and >5 min, respectively (Figure 10). These simulation results are perfectly consistent with the HF Doppler observations.

Kikuchi et al. [1978] and *Kikuchi and Araki* [1979b] showed that the electric potential and currents can be transmitted from the polar ionosphere to the equator at the speed of light by the TM_0 (TEM) mode waves in the Earth-ionosphere waveguide. The TM_0 mode wave has uniform fields in the vertical direction, and so only the TM_0 mode wave has no low cutoff frequency and therefore can propagate unattenuated at all frequencies [*Budden*, 1961]. The TM_0 mode wave is identical to the TEM mode in the two-conductor transmission line. The electric conductivity of the ionosphere is finite, causing some attenuation of the TM_0 mode waves. However, even on the extreme condition of the nighttime low ionospheric conductivity, the attenuation is only 15% for the propagation over 8000 km, which is almost nothing compared with the geometrical attenuation (>90%) due to the small ratio of the size of the polar electric field to the propagation distance [*Kikuchi and Araki*, 1979b].

Kikuchi [2014] constructed the magnetosphere-ionosphere-ground transmission line model composed of two parallel-plane transmission lines to take the field-aligned currents and finite length of the Earth-ionosphere waveguide into the model. It was shown that the TM_0 mode waves in the bounded Earth-ionosphere waveguide achieve quasi-steady ionospheric currents and electric potential distributions with time constants of a few to tens of seconds depending on the ionospheric conductivity. The model well explains the instantaneous onset of the PI over wide latitude ranges on the dayside [*Araki*, 1977] and on the nightside [*Kikuchi*, 1986] and delayed peak times at the dayside equator [*Kikuchi et al*., 1996; *Takahashi et al*., 2015] as well as the delayed phase of the equatorial Pi2 [*Shinohara et al*., 1997]. The waveguide model further explains the upward flow of the Poynting flux from the ionosphere to the magnetosphere as observed on board the spacecraft [*Nishimura et al*., 2010]. On the other hand, the transient times are short enough to allow us to employ the potential solver to calculate the global distribution of the electric potential and currents as was done in the global MHD simulations (Figure 10). To make visible the transmission of the electric potential and currents to the low-latitude ionosphere completed during the MI of SC, we show a schematic diagram in Figure 13, in which the electric potential and currents generated by the dynamo are transmitted to the polar ionosphere by the Alfven waves accompanying the field-aligned currents and to the middle and equatorial latitudes by the TM_0 (TEM) mode waves accompanying the ionospheric currents. Thus, we have the excellent correlations between the upward motion of the ionosphere at midlatitude and the eastward ionospheric currents at the equator (EEJ). The MIG transmission line also explains instantaneous transmission on the nightside, where the electric field is westward as has been observed with the HF Doppler sounder [*Kikuchi et al*., 1985; *Kikuchi*, 1986] and with the electric field measurement onboard ROCSAT [*Takahashi et al*., 2015].

We should emphasize the powerful capability of the HF Doppler sounder to detect the electric field at middle and low latitudes. As shown above, the reflection height is moved by the electric field transmitted from the polar ionosphere with the ionospheric currents, leading to that the capability greatly depends on the reflection condition in the *F* region ionosphere. In particular, the production/loss of the ionization is critical to the Doppler frequency for long-period disturbances [*Tsutsui et al*., 1988]. Nevertheless, the HF Doppler sounder

has been proved powerful to detect the long-period disturbances such as the DP2 and substorms [*Abdu et al*., 1998; *Tsutsui et al*., 1988] as well as the short-period SC, PC, and Pi2.

5. Conclusion

We have shown that the dayside midlatitude ionosphere moves upward when the magnetosphere is compressed. It is also shown that the ionospheric motion is well correlated with the ionospheric currents of the MI that are enhanced at the dayside equator (EEJ). We have shown one event in which the ionospheric motion was initiated by the downward motion, but the electric field absolutely corresponds to the negative EEJ of the PI. These results suggest that the ionosphere is never compressed by the compressional waves but is moved by the potential electric field transmitted with the ionospheric currents from the polar ionosphere. Based on the one-dimensional analytical model, we confirmed that the electric field of the compressional wave is severely suppressed by the conducting ionosphere and ground, and as a result, the ionosphere behaves as an incompressible medium. To confirm the potential electric fields being responsible for the motion of the incompressible ionosphere, we showed that both the PI and MI electric fields are in the opposite direction on the dayside to the nightside. In particular, the electric fields have the evening anomaly with the same direction as in the daytime and enhanced magnitude. To clarify the properties of the electric fields, we reproduced the PI and MI electric fields using the global MHD simulation [*Tanaka*, 2007] that employs the potential solver at the inner boundary of the M-I coupling. The simulated electric fields are consistent with the observations in all respects including the evening anomaly. The simulation results clarified that the evening anomaly is derived from the asymmetric distribution of the global electric potential due to the Hall effects and day-night inhomogeneity of the ionospheric conductivity. To explain the transmission of the electric potential in the incompressible ionosphere, we applied the magnetosphere-ionosphere-ground (MIG) transmission line model [*Kikuchi*, 2014], where the TM_0 (TEM) mode waves transport the electric potential and ionospheric currents at the speed of light. The near-instantaneous transmission achieves the simultaneous motion of the global ionosphere appearing as the incompressible ionosphere. We conclude that the ionosphere is incompressible to the compressional waves during the geomagnetic sudden commencements and that the incompressible ionosphere is moved by the dusk-to-dawn and dawn-to-dusk potential electric fields associated with the ionospheric currents of the PI and MI, respectively.

Acknowledgments

We would like to thank the U.S. NOAA/Weather Service Office at Yap, Ryukyu University, INPE and Federal University of Santa Maria for their help in operating the NICT (National Institute of Information and Communications Technology) space weather monitoring magnetometers at Yap, Okinawa, Sao Luiz, and Santa Maria, respectively. The magnetometers at Kakioka and Kanoya have been operated by the Kakioka Magnetic Observatory, Japan Meteorological Agency, and the data from these stations as well as from Addis Ababa and Tamanrasset have been downloaded from the World Data Center for Geomagnetism, Kyoto. SuperMAG data were obtained from http://supermag.jhuapl.edu/ as daily ASCII files. The HF Doppler sounders have been operated by the University of Electro-Communications. The ACE solar wind data were obtained through the Coordinated Data Analysis Web (CDAWeb). The study of T.K. is supported by the grants-in-aid for Scientific Research (15H05815) of Japan Society for the Promotion of Science (JSPS) and the joint research programs of the Institute for Space-Earth Environmental Research (former Solar-Terrestrial Environment Laboratory), Nagoya University, the Research Institute for Sustainable Humanosphere, Kyoto University, and of the National Institute of Polar Research, Tokyo. The works of T.K. and K.H. are supported by the JSPS KAKENHI grant 26400481(KH), the work of Y.N. by NASA grant NNX15AI62G, NSF grant PLR-1341359, and AFOSR grant FA9550-15-1-0179, and the work of A.S. was supported by the JSPS KAKENHI grant 26400478, 22253006 and the Inter-university Upper atmosphere Global Observation NETwork (IUGONET) project, which is funded by the Ministry of Education, Culture, Sports, Science and Technology (MEXT). The works of TK, YE and BV were supported by the joint research project Indo-Japan project of JSPS, Japan and DST, India (DST/INT/JSPS/P-137/2012).

References

Abdu, M. A., J. H. Sastri, H. Luehr, H. Tachihara, T. Kitamura, N. B. Trivedi, and J. H. A. Sobral (1998), DP 2 electric field fluctuations in the dusk-time dip equatorial ionosphere, *Geophys. Res. Lett.*, *25*(9), 1511–1514, doi:10.1029/98GL01096.

Araki, T. (1977), Global structure of geomagnetic sudden commencements, *Planet. Space Sci.*, *25*, 373–384.

Araki, T. (1994), A physical model of the geomagnetic sudden commencement, in *Solar Wind Sources of Magnetospheric Ultra-Low-Frequency Waves*, *Geophys. Monogr.*, vol. 81, pp. 183–200, AGU, Washington D. C.

Araki, T., J. H. Allen, and Y. Araki (1985), Extension of a polar ionospheric current to the nightside equator, *Planet. Space Sci.*, *33*, 11–16.

Araki, T., K. Keika, T. Kamei, H. Yang, and S. Alex (2006), Nighttime enhancement of the amplitude of geomagnetic sudden commencements and its dependence on IMF-Bz, *Earth Planet. Space*, *58*, 45–50.

Baker, W. G., and D. F. Martyn (1953), Electric currents in the ionosphere I. The conductivity, *Philos. Trans. R. Soc. London, Ser. A*, *246*, 281–294.

Budden, K. G. (1961), *The Wave-Guide Mode Theory of Wave Propagation*, pp. 33–34, Academic Press Inc., London.

Chan, K. L., D. P. Kanellakos, and O. G. Viilard Jr. (1962), Correlation of short-period fluctuations of the Earth's magnetic field and instantaneous frequency measurements, *J. Geophys. Res.*, *67*, 2066–2072, doi:10.1029/JZ067i005p02066.

Davies, K., J. M. Watts, and D. H. Zacharisen (1962), A study of F2-layer effects as observed with a Doppler technique, *J. Geophys. Res.*, *67*, 601–609, doi:10.1029/JZ067i002p00601.

Fujita, S., T. Tanaka, T. Kikuchi, K. Fujimoto, K. Hosokawa, and M. Itonaga (2003a), A numerical simulation of the geomagnetic sudden commencement: 1. Generation of the field-aligned current associated with the preliminary impulse, *J. Geophys. Res.*, *108*(A12), 1416, doi:10.1029/2002JA009407.

Fujita, S., T. Tanaka, T. Kikuchi, K. Fujimoto, and M. Itonaga (2003b), A numerical simulation of the geomagnetic sudden commencement: 2. Plasma processes in the main impulse, *J. Geophys. Res.*, *108*(A12), 1417, doi:10.1029/2002JA009763.

Gjerloev, J. W. (2012), The SuperMAG data processing technique, *J. Geophys. Res.*, *117*, A09213, doi:10.1029/2012JA017683.

Greifinger, C., and P. S. Greifinger (1968), Theory of hydromagnetic propagation in the ionospheric waveguide, *J. Geophys. Res.*, *73*(23), 7473–7490, doi:10.1029/JA073i023p07473.

Hirono, M. (1952), A theory of diurnal magnetic variations in equatorial regions and conductivity of the ionosphere *E* region, *J. Geomagn. Geoelectr. Kyoto*, *4*, 7–21.

Huang, Y.-N. (1976), Modeling HF Doppler effects of geomagnetic sudden commencements, *J. Geophys. Res.*, *81*, 175–182, doi:10.1029/JA081i001p00175.

Huang, Y.-N., K. Najita, and P. Yuen (1973), The ionospheric effects of geomagnetic sudden commencements as measured with an HF Doppler sounder at Hawaii, *J. Atmos. Terr. Phys.*, *35*, 173–181.

Jacobs, J. A., and T. Watanabe (1963), The equatorial enhancement of sudden commencements of geomagnetic storms, *J. Atmos. Terr. Phys.*, *25*, 267–279.

Kanellakos, D. P., and O. G. Villard Jr. (1962), Ionospheric disturbances associated with the solar flare of September 28, 1961, *J. Geophys. Res.*, *67*, 2265–2277, doi:10.1029/JZ067i006p02265.
Kikuchi, T. (1986), Evidence of transmission of polar electric fields to the low latitude at times of geomagnetic sudden commencements, *J. Geophys. Res.*, *91*, 3101–3105, doi:10.1029/JA091iA03p03101.
Kikuchi, T. (2014), Transmission line model for the near-instantaneous transmission of the ionospheric electric field and currents to the equator, *J. Geophys. Res. Space Physics*, *119*, 1131–1156, doi:10.1002/2013JA019515.
Kikuchi, T., and T. Araki (1979a), Transient response of uniform ionosphere and preliminary reverse impulse of geomagnetic storm sudden commencement, *J. Atmos. Terr. Phys.*, *41*, 917–925.
Kikuchi, T., and T. Araki (1979b), Horizontal transmission of the polar electric field to the equator, *J. Atmos. Terr. Phys.*, *41*, 927–936.
Kikuchi, T., and T. Araki (1985), Preliminary positive impulse of geomagnetic sudden commencement observed at dayside middle and low latitudes, *J. Geophys. Res.*, *90*, 12,195–12,200, doi:10.1029/JA090iA12p12195.
Kikuchi, T., T. Araki, H. Maeda, and K. Maekawa (1978), Transmission of polar electric fields to the Equator, *Nature*, *273*, 650–651.
Kikuchi, T., T. Ishimine, and H. Sugiuchi (1985), Local time distribution of HF Doppler frequency deviations associated with storm sudden commencements, *J. Geophys. Res.*, *90*, 4389–4393, doi:10.1029/JA090iA05p04389.
Kikuchi, T., H. Lühr, T. Kitamura, O. Saka, and K. Schlegel (1996), Direct penetration of the polar electric field to the equator during a DP2 event as detected by the auroral and equatorial magnetometer chains and the EISCAT radar, *J. Geophys. Res.*, *101*, 17,161–17,173, doi:10.1029/96JA01299.
Kikuchi, T., S. Tsunomura, K. Hashimoto, and K. Nozaki (2001), Field-aligned current effects on midlatitude geomagnetic sudden commencements, *J. Geophys. Res.*, *106*, 15,555–15,565, doi:10.1029/2001JA900030.
Kivelson, M. G., and D. J. Southwood (1988), Hydromagnetic waves and the ionosphere, *Geophys. Res. Lett.*, *15*(11), 1271–1274, doi:10.1029/GL015i011p01271.
Motoba, T., T. Kikuchi, H. Lühr, H. Tachihara, T.-I. Kitamura, K. Hayashi, and T. Okuzawa (2002), Global Pc5 caused by a DP2-type ionospheric current system, *J. Geophys. Res.*, *107*(A2), 1032, doi:10.1029/2001JA900156.
Nagata, T., and S. Abe (1955), Notes on the distribution of SC* in high latitudes, *Rep. Ionos. Res. Jpn.*, *9*, 39–44.
Nishida, A. (1968), Coherence of geomagnetic DP2 magnetic fluctuations with interplanetary magnetic variations, *J. Geophys. Res.*, *73*, 5549–5559, doi:10.1029/JA073i017p05549.
Nishida, A., N. Iwasaki, and T. Nagata (1966), The origin of fluctuations in the equatorial electrojet; A new type of geomagnetic variation, *Ann. Geophys.*, *22*, 478–484.
Nishimura, Y., T. Kikuchi, A. Shinbori, J. Wygant, Y. Tsuji, T. Hori, T. Ono, S. Fujita, and T. Tanaka (2010), Direct measurements of the Poynting flux associated with convection electric fields in the magnetosphere, *J. Geophys. Res.*, *115*, A12212, doi:10.1029/2010JA015491.
Nopper, R. W., and R. L. Carovillano (1978), Polar equatorial coupling during magnetically active periods, *Geophys. Res. Lett.*, *5*(8), 699–702, doi:10.1029/GL005i008p00699.
Pilipenko, V., E. Fedorov, K. Yumoto, A. Ikeda, and T. R. Sun (2010), An analytical model for Doppler frequency variations of ionospheric HF sounding caused by SSC, *J. Geophys. Res.*, *115*, A10228, doi:10.1029/2010JA015403.
Poole, A. W. V., P. R. Sutcliffe, and A. D. M. Walker (1988), The relationship between ULF geomagnetic pulsations and ionospheric Doppler oscillations: Derivation of a model, *J. Geophys. Res.*, *93*, 14,656–14,664, doi:10.1029/JA093iA12p14656.
Senior, C., and M. Blanc (1984), On the control of magnetospheric convection by the spatial distribution of ionospheric conductivities, *J. Geophys. Res.*, *89*, 261–284, doi:10.1029/JA089iA01p00261.
Shinbori, A., T. Ono, M. Iizima, and A. Kumamoto (2004), SC related electric and magnetic field phenomena observed by the Akebono satellite inside the plasmasphere, *Earth Planet. Space*, *56*, 269–282.
Shinbori, A., Y. Tsuji, T. Kikuchi, T. Araki, and S. Watari (2009), Magnetic latitude and local time dependence of the amplitude of geomagnetic sudden commencements, *J. Geophys. Res.*, *114*, A04217, doi:10.1029/2008JA013871.
Shinohara, M., K. Yumoto, A. Yoshikawa, O. Saka, S. I. Solovyev, E. F. Vershinin, N. B. Trivedi, J. M. Da Costa, and The 210 MM Magnetic Observation Group (1997), Wave characteristics of daytime and nighttime Pi2 pulsations at the equatorial and low latitudes, *Geophys. Res. Lett.*, *24*, 2279–2282, doi:10.1029/97GL02146.
Slinker, S. P., J. A. Fedder, W. J. Hughes, and J. G. Lyon (1999), Response of the ionosphere to a density pulse in the solar wind: Simulation of traveling convection vortices, *Geophys. Res. Lett.*, *26*, 3549–3552, doi:10.1029/1999GL010688.
Spitzer, L., Jr. (1962), *Physics of Fully Ionized Gases*, 39 pp., Dover Publ., Inc., Mineola, New York.
Sutcliffe, P. R., and A. W. V. Poole (1990), The relationship between ULF geomagnetic pulsations and ionospheric Doppler oscillations: Model predictions, *Planet. Space Sci.*, *38*(12), 1581–1589.
Takahashi, N., Y. Kasaba, A. Shinbori, Y. Nishimura, T. Kikuchi, Y. Ebihara, and T. Nagatsuma (2015), Response of ionospheric electric fields at mid-low latitudes during sudden commencements, *J. Geophys. Res. Space Physics*, *120*, 4849–4862, doi:10.1002/2015JA021309.
Tamao, T. (1964), The structure of three-dimensional hydromagnetic waves in a uniform cold plasma, *J. Geomagn. Geoelectr.*, *48*, 89–114.
Tanaka, T. (1995), Generation mechanisms for magnetosphere-ionosphere current systems deduced from a three-dimensional MHD simulation of the solar wind-magnetosphere-ionosphere coupling processes, *J. Geophys. Res.*, *100*, 12,057–12,074, doi:10.1029/95JA00419.
Tanaka, T. (2007), Magnetosphere-ionosphere convection as a compound system, *Space Sci. Rev.*, *133*, 1, doi:10.1007/s11214-007-9168-4.
Tsunomura, S. (1999), Numerical analysis of global ionospheric current system including the effect of equatorial enhancement, *Ann. Geophys.*, *17*, 692–706, doi:10.1007/s00585-999-0692-2.
Tsutsui, M., T. Ogawa, Y. Kamide, H. W. Kroehl, and B. A. Hausman (1988), A method of estimating horizontal vectors of ionospheric electric field deduced from HF Doppler data, *Radio Sci.*, *23*(2), 119–128, doi:10.1029/RS023i002p00119.
Watanabe, T. (1962), Law of electric conduction for waves in the ionosphere, *J. Atmos. Terr. Phys.*, *24*, 117–125.
Wilken, B., C. K. Goertz, D. N. Baker, P. R. Higbie, and T. A. Fritz (1982), The SSC on July 29, 1977 and its propagation within the magnetosphere, *J. Geophys. Res.*, *87*, 5901–5910, doi:10.1029/JA087iA08p05901.

Erratum

In the originally published version of this article, units of some measurements in Table 1 were in error. In addition, equation (12) was mislabeled as equation (11). These errors have since been corrected, and this version may be considered the authoritative version of record.